

Mesenchymal stem cell–mediated ectopic hematopoiesis alleviates aging-related phenotype in immunocompromised mice

*Takayoshi Yamaza,¹ *Yasuo Miura,² Kentaro Akiyama,¹ Yanming Bi,³ Wataru Sonoyama,¹ Stan Gronthos,⁴ WanJun Chen,³ Anh Le,¹ and Songtao Shi¹

¹Center for Craniofacial Molecular Biology, University of Southern California, Los Angeles; ²Graduate School of Medicine, Kyoto University, Kyoto, Japan;

³National Institute of Dental and Craniofacial Research, National Institutes of Health, Bethesda, MD; and ⁴Mesenchymal Stem Cell Group, Division of Haematology, Institute of Medical and Veterinary Science, Adelaide, Australia

Subcutaneous transplants of bone marrow mesenchymal stem cells (BMMSCs) are capable of generating ectopic bone and organizing functional hematopoietic marrow elements in animal models. Here we report that immunocompromised mice received subcutaneous BMMSC transplants using hydroxyapatite tricalcium phosphate as a carrier suppressed age-related degeneration in multiple organs and benefited an increase in life span

extension compared with control littermates. The newly organized ectopic bone/marrow system restores active hematopoiesis via the erythropoietin receptor/signal transducer and activator of transcription 5 (Stat5) pathway. Furthermore, the BMMSC recipient mice showed elevated level of Klotho and suppression of insulin-like growth factor I signaling, which may be the mechanism contributing to the alleviation of aging-like pheno-

types and prolongation of life in the treated mice. This work reveals that erythropoietin receptor/Stat5 pathway contributes to BMMSC-organized ectopic hematopoiesis, which may offer a treatment paradigm of reversing age-related degeneration of multiple organs in adult immunocompromised mice. (Blood. 2009;113:2595-2604)

Introduction

Bone marrow mesenchymal stem cells (BMMSCs) are multipotent postnatal stem cells that are capable of differentiating into a variety of cell types, including osteoblasts, chondrocytes, adipocytes, and muscle cells.¹⁻³ BMMSCs possess the capacity to form new bone and organize hematopoiesis when transplanted subcutaneously into immunocompromised mice using proper carriers.^{1,4-8} The recipient-derived bone/marrow organ structures contain functional hematopoietic stem cells (HSCs), analogous to those from regular bones and are capable of rescuing lethally irradiated mice.⁴ Although it was postulated that multiple factors, including platelet-derived growth factor, basic fibroblast growth factor, and matrix metalloproteinase-9, may be involved in the BMMSC-mediated bone/marrow formation *in vivo*,⁹ the mechanism by which BMMSCs organize and support functional hematopoiesis is unidentified. In addition, the impact of ectopic bone marrow formation to whole body system is unknown. Clinically, BMMSCs have been used for the treatment of a variety of human diseases, including large segmental nonunion bone fractures,¹⁰ severe aplastic anemia,¹¹ and acute graft-versus-host disease,¹² suggesting a feasibility of using BMMSC-organized hematopoietic progenitor source for stem cell–based clinical therapies.

Recent animal studies have attributed certain growth factors, calorie restriction, genetic pathways, and immunity as mechanisms contributory to aging and longevity.¹³⁻¹⁸ Insulin and insulin-like growth factor-I (IGF-I) pathways have been considered as an evolutionarily conserved mechanism associated with altered life span.^{15,16} Disruption of the insulin and IGF-I signaling pathways significantly extends life span in several animal models, whereas

decreased circulation of IGF-I levels and/or signaling play a key role in delayed aging and prolonged longevity.¹⁹ Other studies suggested that the altered level of growth hormone, insulin, and IGF-5 or downstream signaling molecules of the insulin/growth hormone/IGF-I axis may regulate aging and longevity.²⁰⁻²² Recently, a study in mice showed that overexpression of Klotho, a circulating hormone that inhibits intracellular insulin and IGF-I signaling, can alleviate aging-like phenotypes and extend life span in both sexes independent of caloric restriction and body growth.¹⁸

In this study, we found that erythropoietin receptor (EPO-R) is a surface molecule for progenitors of BMMSCs. The EPO-R/signal transducer and activator of transcription 5 (Stat5) pathways contribute to BMMSC-mediated hematopoietic organization and mobilization, which may benefit adult immunocompromised mice from age-related degeneration in multiple organ systems and an increase in life span.

Methods

Mice

Littermate female Beige Nude XidIII (*nu/nu*) immunocompromised mice and enhanced green fluorescent protein (eGFP) transgenic mice were purchased from Harlan (Indianapolis, IN). C3H/HeJ mice were from The Jackson Laboratory (Bar Harbor, ME). Animal experiments were performed under the research protocol approved by the Institutional Animal Care and Use Committee of the University of Southern California (protocol 10874). All animals were maintained in a temperature-controlled room with

Submitted October 2, 2008; accepted December 7, 2008. Prepublished online as *Blood* First Edition paper, December 12, 2008; DOI 10.1182/blood-2008-10-182246.

*T.Y. and Y.M. contributed equally to this work.

The online version of this article contains a data supplement.

The publication costs of this article were defrayed in part by page charge payment. Therefore, and solely to indicate this fact, this article is hereby marked "advertisement" in accordance with 18 USC section 1734.

a 12-hour alternating light-dark cycle and fed sufficient diet and water ad libitum throughout the experimental period.

Antibodies

Antiserum against STRO-1 was treated as reported previously.²³ The other antibodies used in this study are described in Document S1 (available on the *Blood* website; see the Supplemental Materials link at the top of the online article).

Isolation and culture of human BMMSCs

BMMSCs were isolated from human whole bone marrow aspirates and cultured as described previously.^{24,25} All human material was obtained with informed consent in accordance with the Declaration of Helsinki. Detailed methods are described in Document S1.

Transplantation of BMMSCs and human skin fibroblasts into immunocompromised mice

Subcutaneous transplantation of BMMSCs was performed on 6-month-old immunocompromised mice as described previously.^{24,25} Detailed methods are described in Document S1. Age-matched immunocompromised mice were used as experimental controls. Additional control groups included subcutaneous transplantation of hydroxyapatite tricalcium phosphate (HA/TCP) carrier in the presence or absence of human skin fibroblasts (FBs). Isolation and culture of FBs are described in Document S1. We also included a control of bone marrow transplantation group using the standard intravenous infusion approach. Briefly, mice were separately housed and routinely monitored for daily activities and health status. All mice were maintained under routine monitor until spontaneous death. Eight weeks after the transplantation, BMMSC (n = 3) and FB (n = 3) transplanted immunocompromised mice were harvested to collect transplants. Fourteen-month-old immunocompromised mice with BMMSC transplants (n = 3) were randomly selected for bromodeoxyuridine (BrdU) label-retaining assay. At 16 months of age, BMMSC-transplanted (n = 3) and the age-matched control (n = 3) immunocompromised mice were selected randomly and harvested of organ tissues, cells, peripheral blood and urine, and measurement of biomarkers. These mice were not counted for survival analysis.

rhEPO treatment

BMMSCs (0.5×10^6) were seeded on a 100-mm tissue culture dish and cultured. After reaching optimal condition, recombinant human EPO (rhEPO, 0.1 U/mL, R&D Systems, Minneapolis, MN) was added. Total protein was collected at indicated times. EPO-treated (EPO⁺) and non-treated (EPO⁻) BMMSCs were harvested for flow cytometric analysis and subcutaneous transplantation with HA/TCP as a carrier into 8-week-old immunocompromised mice. Eight weeks after transplantation, 3 transplants from each group were harvested and analyzed.

Small interfering RNA (siRNA) transfection

Human EPO-receptor, Stat5, and control siRNAs (Santa Cruz Biotechnology, Santa Cruz, CA) were transfected into BMMSCs as described in Document S1. Total protein was extracted for Western blot analysis. siRNA-treated BMMSCs were transplanted with HA/TCP as a carrier into 8-week-old immunocompromised mice. Eight weeks after transplantation, 3 transplant tissues were harvested from each group.

BrdU label-retaining assay

BrdU (50 mg per g body weight; Sigma-Aldrich, St Louis, MO) was injected intraperitoneally twice daily for 3 days into 14-month-old immunocompromised mice, which received BMMSC transplants at 6 months of age. Fourteen weeks after the injection, the transplants were harvested. BrdU-labeled cells were detected on the paraffin-embedded sections using a BrdU Staining Kit (Invitrogen, Carlsbad, CA) according to the manufacturer's instructions.

HSC homing and releasing assay

Bone marrow cells were collected from femurs and tibias of eGFP mice. The cells (10^6) were intravenously injected into 8-week-old female immunocompromised mice (n = 3) that initially received BMMSC transplants for 8 weeks. Four weeks after injection, BMMSC transplants were removed and retransplanted subcutaneously into secondary recipient 8-week-old female immunocompromised mice (n = 3). Age-matched nontransplanted mice (n = 3) were used as negative controls. The peripheral blood was collected 4 weeks after secondary transplantation for analysis of eGFP⁺ leukocytes by flow cytometry.

Micro-computed tomography and peripheral quantitative computed tomography analyses

Micro-computed tomography and peripheral quantitative computed tomography analyses were performed using lumbar vertebra of 16-month-old immunocompromised mice as reported previously.²⁵ Detailed methods are described in Document S1.

Histology, immunohistochemistry, histochemistry, and histometry

Brain, bone (femur, tibia, and lumbar vertebra), liver, and skin tissues were harvested from 16-month-old immunocompromised mice. Transplant tissues were harvested at the indicated period. All samples were fixed with 4% paraformaldehyde. Bone and transplant samples were decalcified with 10% ethylenediaminetetraacetic acid. All samples were dehydrated and embedded in paraffin; 6- μ m sections were cut and dewaxed. Sections were stained with hematoxylin and eosin. Some sections were used for immunostaining, tartrate-resistant acid phosphatase (TRAP), or terminal deoxynucleotidyl transferase biotin-dUTP nick end labeling staining (Document S1). Histometric analysis and quantitation of area (new bone area, bone marrow/niche area, alizarin red-positive area, total area) and cell number (immunopositive cell number, TRAP-positive cell number, total cell number) were determined using National Institutes of Health (NIH) ImageJ from 5 to 7 images per each sample,²⁴ followed by the mean calculation. The data were averaged in each experimental group. The intra-experimental group differences were calculated as mean values.

Blood glucose, serum, and urine assay

Measurement of glucose level in peripheral blood is described in Document S1. We quantified serum levels of IGF-I, C-terminal telopeptides of type I collagen, osteoprotegerin (OPG), and receptor activator of nuclear factor- κ B ligand (RANKL) by enzyme-linked immunosorbent assay (ELISA) using commercial kits following the manufacturer's instructions (Document S1). Serum Klotho level was measured as described in Document S1. Urine protein was measured by the Bradford method using Bio-Rad Protein Assay (Bio-Rad, Hercules, CA) according to the manufacturer's instructions. Each assay was measured in triplicate per each subject. The results were averaged in each group. The intragroup differences were calculated as mean values.

Isolation and culture of mouse BMMSCs

mBMMSCs were isolated and cultured as previously reported.²⁵ Detailed methods are described in Document S1.

Colony-forming unit fibroblast assay

We performed colony-forming unit fibroblast (CFU-F) assay as described previously.²⁵ Cell clusters containing more than 50 cells were counted as a colony under light microscopy according to the previous study.²⁵ Detailed methods are described in Document S1.

Cell proliferation assay

We performed CFU-F assay as described previously.²⁵ Detailed methods are described in Document S1.

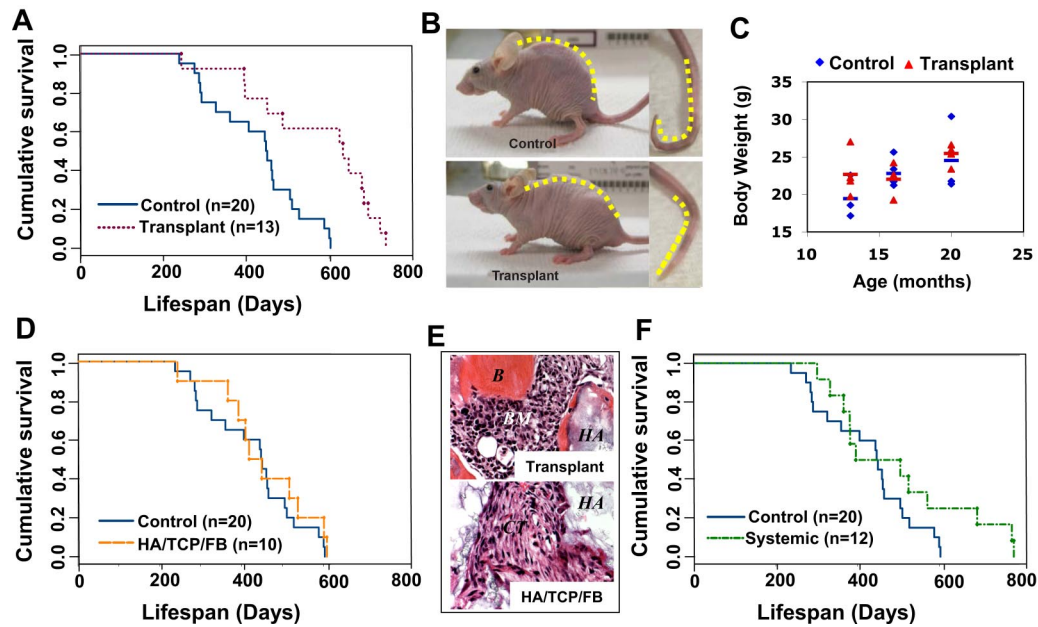


Figure 1. Subcutaneous transplantation of human BMMSCs extends life span in immunocompromised mice. (A) Kaplan-Meier analysis of survival. Recipient mice transplanted with subcutaneous human BMMSC using HA/TCP as a carrier vehicle (Transplant, $n = 13$) manifested a significantly increased life span compared with age-matched control immunocompromised mice (Control, $n = 20$; $P < .05$). (B) The natural aging phenotype of human kyphosis was observed in 6 of 9 aging control mice, shown here as extreme curvature of the vertebrae and tail, although not in transplantation mice ($n = 15$). (C) Body weight at indicated months showed no significant difference between control and transplant recipients. Bars represent the means. (D) When human skin fibroblasts were transplanted subcutaneously using HA/TCP as a carrier (HA/TCP/FB), there is no increased life span in the recipients ($n = 10$; $P = .391$). (E) Newly formed bone (B) and bone marrow (BM) were found in the BMMSC transplants (Transplant) at 8 weeks after transplantation. However, the fibroblast group (HA/TCP/FB) failed to form new tissue and only showed connective tissue (CT) around HA/TCP particles (HA) by hematoxylin and eosin staining. (F) When human BMMSCs (10^6) were infused into immunocompromised mice ($n = 12$) via tail vein, there was no consistent increase in life span extension ($P > .05$) compared with the control group.

Population doubling assay

We performed population doubling assay according to previous report.²⁵ Detailed methods are described in Document S1.

In vitro osteogenic assay

BMMSCs were cultured for osteogenic induction as previously reported.²⁵ The calcium deposits were identified using alizarin red staining.²⁵ Alizarin red-positive and total area were measured using NIH Image J from 5 to 7 images per each sample, followed by the mean calculation. The data were averaged in each experimental group.^{24,25} The intraexperimental group differences were calculated as mean values.

In vivo osteogenic assay

mBMMSCs (2.0×10^6) were implanted subcutaneously with HA/TCP as a carrier into 8-week-old immunocompromised mice. Eight weeks after transplantation, the transplants were harvested.

Flow cytometric analysis

We immunostained cells for flow cytometry as described previously²⁴ (Document S1) and analyzed using a FACSCalibur flow cytometer (BD Biosciences, San Jose, CA).

RT-PCR analysis

cDNA was obtained from total RNA extracted from cultured cells and amplified (Document S1). The specific primer pairs for human EPO-R and glyceraldehyde 3 phosphate dehydrogenase were as follows: EPO-R (GenBank accession no. NM_000121²⁶), sense: 5'-GAGCATGCCAGGAT-ACCTA-3' (nucleotides 1220-1239), antisense: 5'-TACTCAAAGCTG-GCAGCAGA-3' (nucleotides 1394-1413); glyceraldehyde 3 phosphate dehydrogenase (GenBank accession no. M33197²⁷), sense: 5'-CTGGCCTC-CAGCTACATCTC-3' (nucleotides 12-31), antisense: 5'-TCATATTTG-GCAGTTTTTCT-3' (nucleotides 807-827).

Western blot analysis

Western blot analysis was followed as in a previous study.²⁴ Detailed methods are described in Document S1.

Statistical analysis

Student *t* test and Mantel-Haenszel test were used to analyze significance between 2 groups. *P* values less than .05 were considered significant. Kaplan-Meier was used for survival curve analysis.

Results

Ectopic BMMSC transplantation extends life span in immunocompromised mice

In this study, we revealed that transplantation of BMMSCs with HA/TCP as a carrier subcutaneously into 6-month-old immunocompromised mice significantly extends life span, compared with age-matched control mice (Figure 1A). We analyzed survival using the Mantel-Haenszel test and found significantly greater overall survival of transplant recipient mice compared with their littermates. The mean time to death was 355.7 plus or minus 74.5 days in 50% of control mice and 461.0 plus or minus 137.8 days in 50% of transplant recipients. It appeared that the longevity of the recipient mice transplanted with BMMSC was significantly improved with an average extension of life span by 33.4% ($P < .01$). Notably, we observed an alleviation of a common natural aging process, shown here in 6 of 9 control mice at 16 months of age, as a reduction in the vertebral curvature of the backs and the tails (Figure 1B). These aging phenotypes were absent in all survived BMMSC-transplanted mice (Figure 1B). Because caloric restriction is associated with increased longevity, we monitored food

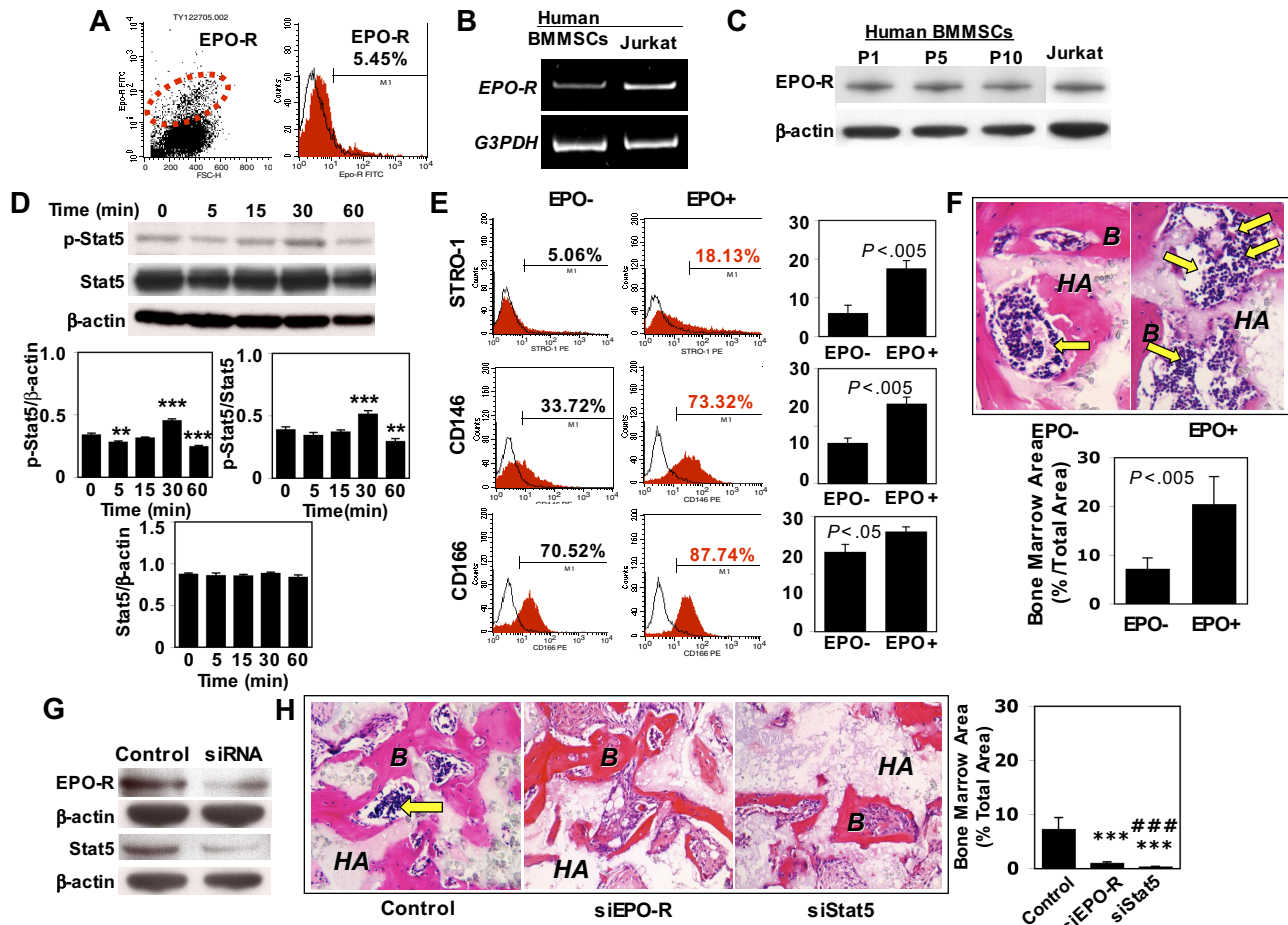


Figure 2. EPO-R is a progenitor marker of human BMMSCs and mediates bone marrow organization in vivo. (A) Flow cytometric analysis revealed that a small percentage (5.45%) of BMMSCs expressed EPO-R. (B) RT-PCR analysis confirmed EPO-R gene expression in BMMSCs. Jurkat cells were used as a positive control for EPO-R expression. (C) Western blot analysis further confirmed that BMMSCs express EPO-R at passages 1, 5, and 10 (P1, P5, and P10). (D) rhEPO treatment (0.1 U/mL) for the indicated time (minutes) induced a significantly up-regulated expression of phospho-Stat5 in BMMSCs at 30 minutes compared with either β -actin or Stat5 ($n = 3$). However, expression level of Stat5 showed no significant change ($n = 3$). (E) STRO-1⁺, CD146⁺, and CD166⁺ BMMSCs were significantly increased in the rhEPO treatment group (EPO⁺) compared with the untreated group (EPO⁻; $n = 3$). (F) rhEPO (0.1 U/mL)-treated BMMSCs (EPO⁺) were capable of inducing active hematopoietic marrow formation (arrows) when transplanted into immunocompromised mice with HA/TCP (HA) as assessed by hematoxylin and eosin staining. B indicates bone. Original magnification $\times 400$. Bars represent SD (EPO⁺, $n = 3$; EPO⁻, $n = 3$). Semiquantitative analysis showed that EPO treatment resulted in a significantly increased bone marrow formation in the BMMSC transplants compared with untreated control BMMSCs. (G) Western blotting analysis confirmed a significant inhibition of EPO-R and Stat5 expression in BMMSCs transfected with siRNA targeting EPO-R and Stat5, respectively. (H) Loss of function of EPO-R and Stat5 resulted in inhibition of bone marrow (arrow) formation in 8-week-old BMMSC transplants compared with the nonspecific siRNA-transfected transplant (Control). HA indicates HA/TCP. Original magnification $\times 200$. Bars represent SD (Control, $n = 3$; EPO-R, $n = 3$; Stat5, $n = 3$; *** $P < .005$ vs Control; # $P < .05$ vs EPO-R; ### $P < .005$ vs EPO-R).

intake and oxygen consumption in both groups (data not shown). No significant differences in body weight between BMMSC-transplanted and control mice were observed (Figure 1C), suggesting that the life span extension may be independent of food intake and weight. To confirm the specific effect of transplantation of BMMSC/HA/TCP in life span extension in immunocompromised mice, we transplanted HA/TCP particle with and without skin fibroblasts and found no significant differences in life span compared with control immunocompromised mice (Figures 1D and S1). As expected, HA/TCP carrier with and without fibroblast transplants showed absence of ectopic bone/marrow organization compared with BMMSC/HA/TCP transplants (Figure 1E). To further confirm that the effect on life span extension was associated with an organized BMMSC-hematopoietic organ, we treated mice with the intravenous infusion of BMMSCs, the BMMSC-infused mice failed to generate an organized hematopoietic organ and did not benefit a significant increase in survival as seen in the subcutaneous BMMSC/HA/TCP transplantation group (Figure 1F). These findings suggest that subcutaneous transplantation of

BMMSC/HA/TCP is capable of establishing an organized hematopoietic marrow organ that may contribute to the physiologic process leading to life span extension in immunocompromised mice.

EPO-R/Stat5 axis regulates BMMSC-organized ectopic hematopoietic marrow formation

Because the generation of an organized bone/hematopoietic marrow organ appears essential in the survival benefit in BMMSC/HA/TCP transplantations, we examined the mechanisms underlying BMMSC-mediated recipient hematopoietic marrow formation. First, we found that 5.45% of the culture expanded BMMSCs expressed EPO-R by flow cytometric analysis (Figure 2A). The EPO-R-positive BMMSCs may represent a small subset of the heterogeneous population of BMMSCs, an inherent feature of mesenchymal stem cells as reported previously.^{3,5,6} Subsequently, we confirmed that BMMSCs expressed EPO-R by reverse-transcription polymerase chain reaction (RT-PCR) and Western

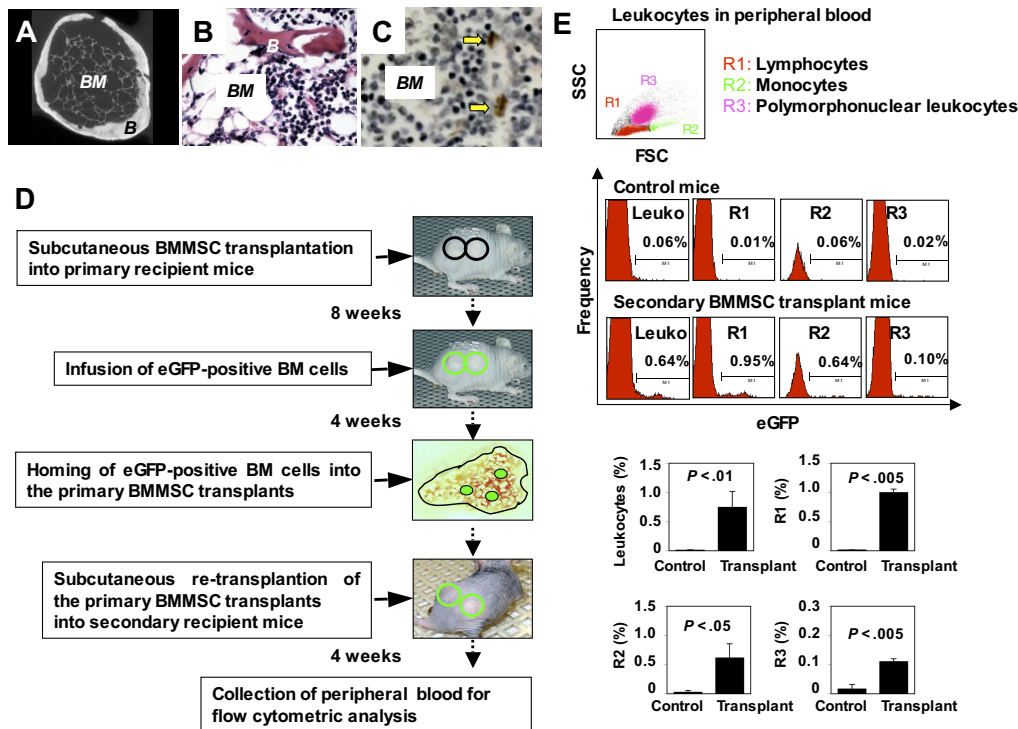


Figure 3. Subcutaneous transplantation of human BMMSCs reconstitutes active hematopoiesis in adult immunocompromised mice. (A) Micro-computed tomography analysis revealed that bone (B) and bone marrow elements (BM) regenerated in 8-week BMMSC transplants. Original magnification $\times 200$. (B,C) Long-term (12 months) engraftment of BMMSC-mediated bone/marrow formation in subcutaneous transplants showing organized bone (B) and bone marrow components (BM) by hematoxylin and eosin staining (B) and BrdU label retaining assay showing BrdU-positive cells (arrows) in the bone marrow (BM) compartment for 14 weeks after labeling (C). Original magnification $\times 200$. (D) A scheme of eGFP⁺ mouse bone marrow (BM) cells homed to the BMMSC-generated bone/marrow organs. BMMSCs were transplanted subcutaneously into immunocompromised mice (top panel). Eight weeks after transplantation, eGFP⁺ BM cells were injected through the tail vein of the primary transplant recipient (second top panel). The eGFP⁺ BM cells homed to the bone marrow niche in the primary BMMSC transplants (third top panel). Four weeks later, the primary BMMSC transplants were removed as donor transplants for secondary transplantation (fourth top panel). Four weeks after secondary transplantation, peripheral blood was collected for flow cytometric analysis (bottom panel). (E) The secondary transplantations were capable of supplying hematopoietic cells in the circulation of the recipients ($n = 3$) at 4 weeks after transplantation. Flow cytometric analysis revealed the existence of eGFP⁺ lymphocytes, monocytes, and polymorphonuclear leukocytes in peripheral blood leukocytes (PBLs). PBLs of the nontransplanted mice were used as negative controls. An average of 3 mice per group was used in the analysis of each cell subset. Comparative analysis of each cell subset was determined and statistically analyzed (Control, $n = 3$; Transplant, $n = 3$; leukocyte percentage, $P < .01$; R1, $P < .005$; R2, $P < .05$; R3, $P < .005$). Data are representative of 3 independent experiments.

blot analysis (Figure 2B,C). When treated with EPO, BMMSCs showed a significant activation of Stat5 phosphorylation at 30 minutes of induction, representing a conservation of the traditional EPO/EPO-R/Stat5 pathway in BMMSCs (Figure 2D). However, expression of Stat5 in BMMSCs was not altered by EPO (Figure 2D). Treatment with EPO led to the up-regulated expression of mesenchymal stem cell markers STRO-1, CD146, and CD166 (Figure 2E) and level of EPO-R (Figure S2C), suggesting a possible role of EPO-R in the regulation of stem cell markers in BMMSCs. Moreover, we found that EPO-stimulated BMMSC proliferation and improved cell viability as assessed by BrdU labeling and cell viability test, respectively (Figure S2A,B). Using the *in vivo* transplantation approach, we found that EPO-treated BMMSCs showed a 2- to 3-fold increased capacity of organizing recipient bone marrow elements (Figure 2F). When EPO-R or Stat5 were knockdown using siRNA approach (Figure 2G), the capacity of organizing hematopoietic bone marrow was significantly decreased, approximately 8- and 25-fold reduction in the percentage of bone marrow area, respectively (Figure 2H). Given that EPO and EPO-R systems showed diverse biologic functions in hematopoietic and nonhematopoietic systems,²⁸ our data provided further evidence that EPO receptor is an early marker of BMMSCs and the EPO/EPO-R/Stat5 signaling pathway contributes in part to mechanisms underlying transplanted BMMSC-organizing hematopoiesis.

Reconstitution of active hematopoiesis in immunocompromised mice

Because subcutaneous transplantation of human skin fibroblasts using HA/TCP as a carrier failed to extend life span in immunocompromised mice, we hypothesized that BMMSC-mediated ectopic bone/marrow organization can restore active hematopoiesis and alleviate age-related degeneration in recipient mice. First, *ex vivo*-expanded BMMSCs were transplanted into the dorsal surface of immunocompromised mice. At 8 weeks after transplantation, bone/marrow organ-like structures were generated (Figure 3A). Newly formed bone/hematopoietic marrow components persisted as long as 18 months as assessed by hematoxylin and eosin staining (Figure 3B) and presence of long-term retaining (14 weeks) BrdU-positive cells in the marrow compartment (Figure 3C), suggesting that the transplanted BMMSC-organized bone/marrow system is capable to persist throughout the whole course of the after transplant period and may contribute, to some extent, to the immediate niche of stem/progenitor cell populations. To further examine the homing and long-term engraftment of BMMSC transplant in our system, whole bone marrow cells derived from eGFP transgenic mice were administered through the tail vein of primary recipient mice at 8 weeks after subcutaneous BMMSC transplantation (Figure 3D). The primary BMMSC transplants generated in immunocompromised recipients, capable of homing

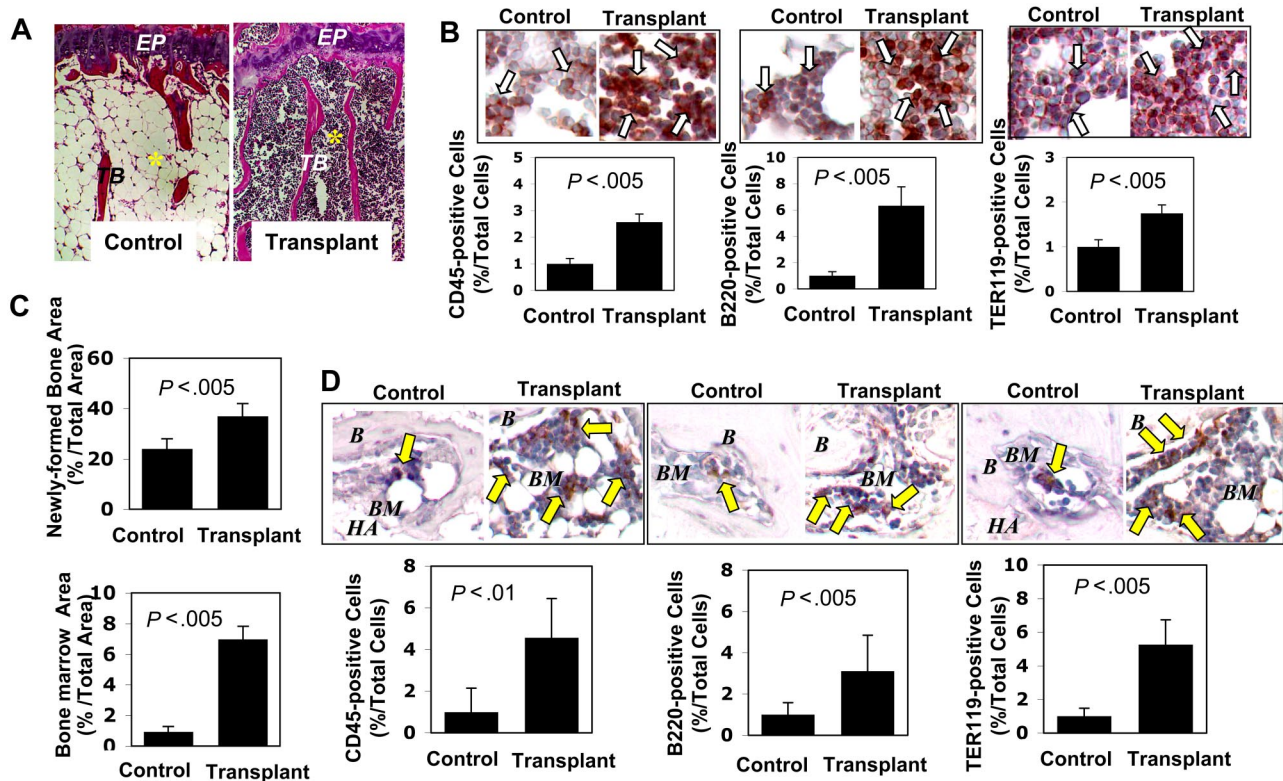


Figure 4. Subcutaneous transplantation of human BMMSCs rescues bone marrow elements. (A) Representative femur sections showed increment of trabecular bone in 3 BMMSC transplant recipient mice at 16 months of age (Transplant) compared with the untreated age-matched littermates (Control; $n = 3$). Abundant red marrow elements, characteristic of increased hematopoietic cells, were observed in the transplant recipients compared with the fatty, acellular marrow compartment in the control mice. EP indicates epiphyseal cartilage; TB, trabecular bone. *Bone marrow. Original magnification $\times 200$. (B) Immunohistochemical staining showed numerous CD45⁺, B220⁺, and TER119⁺ cells (open arrows) in the femur bone marrow of recipient mice (Transplant, $n = 3$) compared with the age-matched control mice (Control, $n = 3$). Bars represent SD. (C) BMMSCs isolated from mice that received subcutaneous BMMSC transplants ($n = 3$) were transplanted into new immunocompromised recipient mice using HA/TCP (HA) as a carrier. At 8 weeks after transplantation, the transplants showed significantly increased bone (top panel) and bone marrow (bottom panel) formation compared with the BMMSC transplants from control mice ($n = 3$). Bars represent SD. (D) Immunohistochemical staining showed increased CD45⁺, B220⁺, and TER119⁺ cells (arrows) in the ectopic bone marrow compartment (BM) generated by BMMSCs from the mice received subcutaneous BMMSC transplants (Transplant; $n = 3$) compared with the ectopic bone marrow compartment (BM) generated by BMMSCs from regular mice (Control, $n = 3$). B indicates bone; HA, HA/TCP. Bars represent SD.

eGFP bone marrow cells,⁴ were reimplanted into the dorsal surface of secondary immunocompromised recipient mice (Figure 3D). Four weeks later, leukocytes in the peripheral blood of the secondary recipient mice were analyzed. Flow cytometric analysis revealed a 75-fold increase in eGFP⁺ leukocytes (0.64%) in the peripheral blood consisting of both lymphoid (R1, 0.95%) and myeloid cells (monocytes, R2, 0.64% in eGFP⁺ leukocytes; polymorphonuclear cells, R3, 0.10% in eGFP⁺ leukocytes) in secondary transplantation compared with control mice (Figure 3E). The marked systemic leukocytic elevation was consistent with similar increase in both lymphoid and myeloid components (Figure 3E). These results indicated that transplanted BMMSCs could yield long-term engrafting mesenchymal stem cells with capability to organize marrow elements, reconstitute active hematopoiesis, and mobilize functional hematopoietic components in the recipients.

To determine whether active hematopoiesis occurs in other bones while the activity presumably slows down after growth spurt, we examined the femurs and vertebrae in 3 mice from each group at age 16 months. In 12 of 15 sections of 3 BMMSC transplant recipients, we found that the femur showed distinct red and cellular marrow compartment in transplant recipient mice versus the expected yellow and fatty marrow in the normal aging control mice (Figure 4A). The red marrow component is enriched in CD45⁺ hematopoietic cells (2- to 3-fold increase), B220⁺ B cells (6- to 7-fold), and TER119⁺ erythroid cells (~ 2 -fold) (Figure 4B). Moreover, we found that BMMSCs

derived from the primary transplant recipient mice showed an elevated bone (~ 2 -fold) and bone marrow formation (7- to 8-fold) when subcutaneously transplanted into secondary recipient immunocompromised mice (Figure 4C). Bone marrow section of the secondary recipient mouse showed an increase in CD45⁺ hematopoietic cells (4- to 5-fold), B220⁺ B cells (3- to 4-fold), and TER119⁺ erythroid cells (5- to 6-fold) compared with those in controls (Figure 4D). Although BMMSC transplant recipient mice showed no elevated EPO level in serum, their BMMSCs exhibited increased expression level of EPO-R compared with control BMMSCs (Figure S2D,E). These data suggest that BMMSCs are capable of reorganizing functional hematopoietic marrow elements and reconstituting active medullary hematopoiesis at the transplantation site, and possibly, other bones, in this case the femur. The hematopoietic contribution from the extramedullary process such as spleen is probable, based on the histologic feature of enlargement of the germinal center in the white pulp (Figure S3G). However, further studies are needed to confirm its hematopoietic composition. Taken together, the reestablishment of active hematopoiesis in adult mice, an early developmental process that slows down or diminishes in the aging process, reveals a practical approach of using BMMSC-mediated reconstitution of active hematopoiesis to boost the immune system or rescue the inherent immunologic impairment in immunocompromised mice.

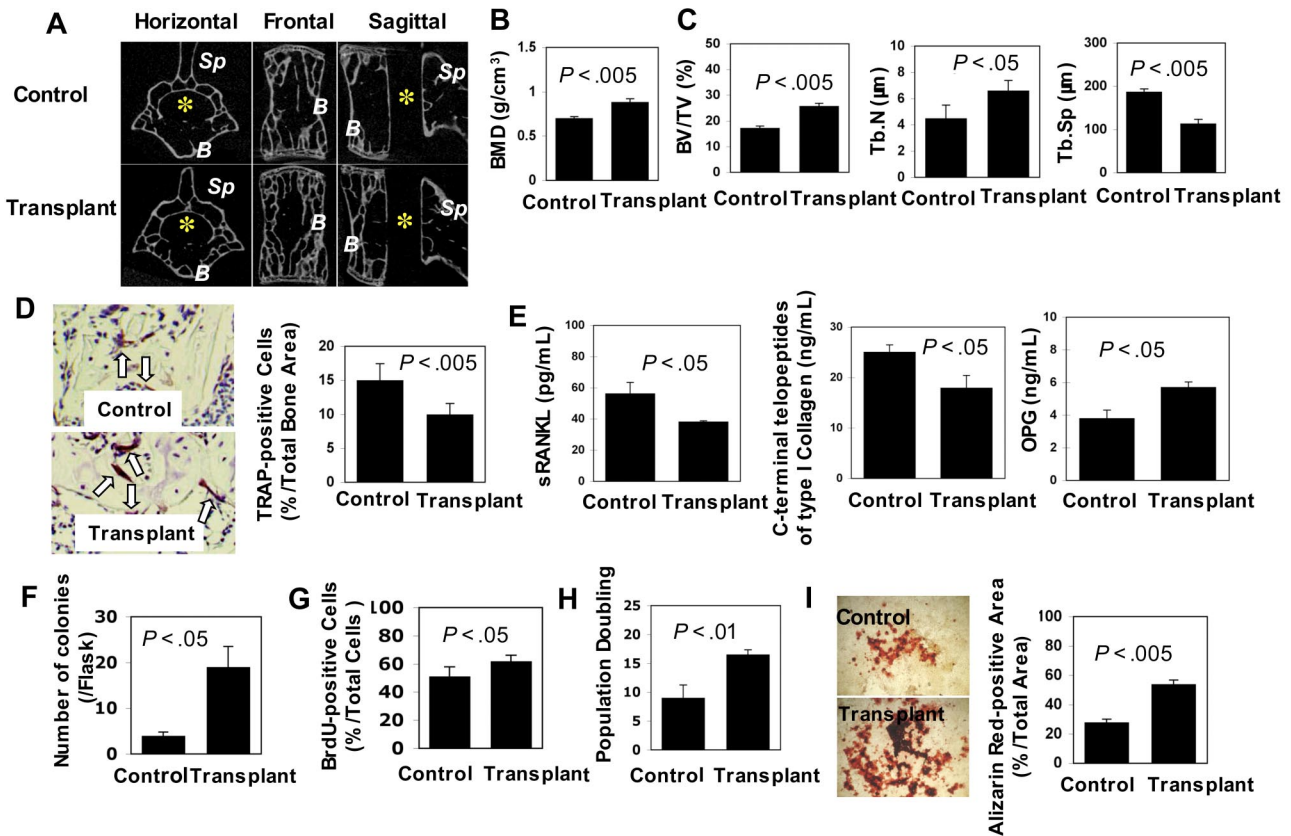


Figure 5. Subcutaneous transplantation of human BMMSCs rescues bone loss. (A) Micro-computed tomography analysis revealed that the third lumbar vertebra in transplant recipient mice (Transplant, lower panels) at 10 months after transplantation showed increase in trabecular bone volume compared with that of age-matched control mice (Control, top panels). *B* indicates vertebral body; *Sp*, spinous process of vertebra. *Vertebral foramen. (B) Bone mineral density (BMD) of femurs in recipient mice (Transplant, $n = 3$) was significantly improved compared with age-matched controls (Control, $n = 3$), as assessed by dual X-ray absorptiometry analysis. Bars represent SD. (C) Bone morphologic analysis demonstrated increase in bone volume versus total volume (BV/TV) and trabecular number (Tb.N) and decrease in trabecular separation (Tb.Sp) in recipient mice (Transplant, $n = 3$) compared with the controls (Control, $n = 3$). Bars represent SD. (D) The number of TRAP-positive cells (arrows) decreased in the vertebral body of recipient mice (Transplant, $n = 3$) compared with control mice (Control, $n = 3$). Original magnification $\times 400$. Bars represent SD. (E) ELISA assay revealed that serum sRANKL and C-terminal telopeptides type I collagen were decreased in recipient mice (Transplant, $n = 3$) compared with control mice (Control, $n = 3$). However, OPG was markedly increased in the recipient mice. Bars represent SD. (F) The number of CFU-F of BMMSCs derived from the recipient mice (Transplant, $n = 3$) increased compared with the age-matched control (Control, $n = 3$). Bars represent SD. (G) The proliferation of recipient BMMSCs (Transplant, $n = 3$) was significantly increased compared with the control group ($n = 3$), as determined by BrdU incorporation assay. Bars represent SD. (H) The population doublings of BMMSCs from recipient mice (Transplant, $n = 3$) were significantly increased compared with control mice (Control, $n = 3$). Bars represent SD. (I) Alizarin red staining showed that BMMSCs derived from recipient mice (Transplant, $n = 3$) had higher calcium accumulation than that from control mice (Control, $n = 3$) under osteogenic conditions. Bars represent SD.

Alleviating aging-like phenotypes in multiple organ systems

Given that BMMSC-mediated hematopoietic marrow formation participates in the immune system, we hypothesized that subcutaneous BMMSC transplantation may contribute to life span extension by retarding the age-related degenerative processes in multiple organs in transplant recipients. We first examined the bone/marrow system using histologic and functional analyses. Increased trabecular bone volume (~ 2 -fold) and bone mineral density were observed in both vertebrae and femurs of 3 transplant recipient mice as assessed by micro-computed tomography and dual X-ray absorptiometry analysis, respectively (Figure 5A-C). In addition, we observed an overall suppression of osteoclastic activity in the vertebra of the recipient mice evidenced by decreased TRAP-positive osteoclasts (~ 0.5 -fold; Figure 5D), reduced levels of soluble RANKL (sRANKL; ~ 0.5 -fold) and C-terminal telopeptides of type I collagen (~ 0.5 -fold) and increased level of OPG (~ 2 -fold) compared with the control littermates (Figure 5E). These data suggest that BMMSC transplantation may slow down the aging-related osteoporosis process by enhancing osteogenesis and suppressing osteoclast activity.

Next, we examined whether BMMSC transplantation affected mesenchymal stem cell functions of the recipients. By examining the CFU-F efficiency of BMMSCs from 3 recipients, an assay representing the number of clonogenic mesenchymal progenitors, we found a significantly increased number of CFU-F in 3 recipient mice compared with the untreated control mice (4-fold; Figure 5F). In addition, the proliferation and population doublings of BMMSCs from the recipient mice were also dramatically increased compared with the control group, as assessed by BrdU incorporation (~ 1.5 -fold) and ex vivo proliferation analysis (~ 2 -fold; Figure 5G,H). Moreover, we showed that subcutaneous BMMSC transplantation led to advanced osteogenic differentiation of the recipient BMMSCs, as shown by increased mineralization in osteogenic inductive cultures (~ 2 -fold; Figure 5I). Taken together, these data indicate that subcutaneous transplantation of BMMSC could enhance stem cell functions in the recipients.

In the cutaneous organ, we observed significant rejuvenating features in the skin of 3 recipient mice, including an overall increased cell number and thickness of the epidermis (~ 3 -fold; Figure S3A,B), increased sebaceous glands (2-fold; Figure S3C), and increased cell proliferation in epidermis and sebaceous glands

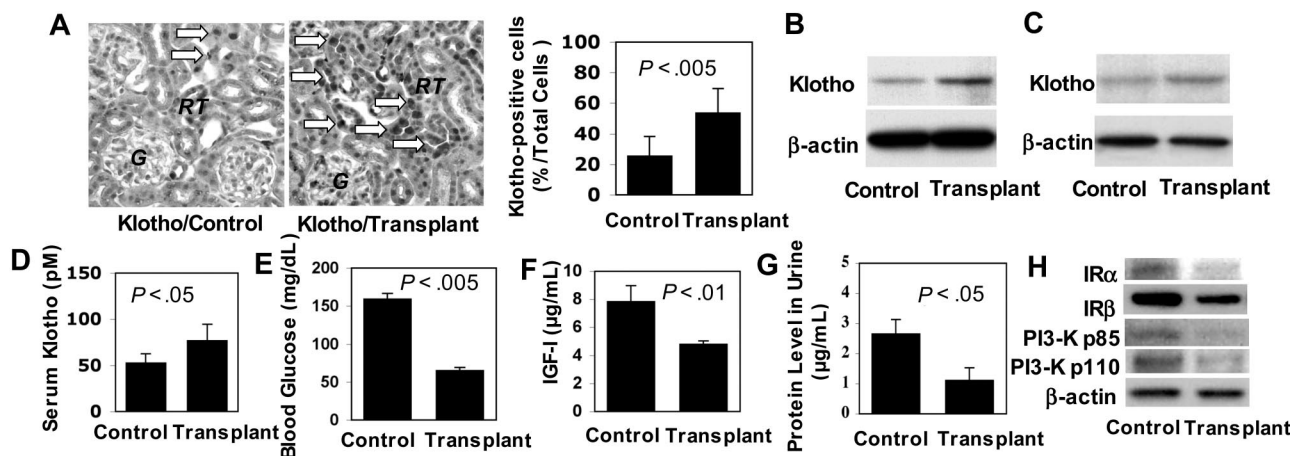


Figure 6. Subcutaneous human BMMSC transplantation up-regulated Klotho expression in immunocompromised mice. (A) Immunohistochemical staining with anti-Klotho antibody showed that transplant recipient mice (Transplant) expressed higher level of Klotho (\Rightarrow) in the epithelial cells of the renal tubules (RT) than those of age-matched controls (Control). G indicates glomerulus. Original magnification $\times 200$. Bars represent SD. (B) Western blot analysis confirmed that Klotho was elevated in kidney of transplant recipient (Transplant, $n = 3$) compared with nontreated littermates (Control, $n = 3$). (C) Likewise, Western blot analysis showed elevated Klotho in brain of transplant recipient mice (Transplant $n = 3$) compared with the Control ($n = 3$). (D) ELISA assay further confirms elevated serum Klotho level in transplant recipient mice (Transplant, $n = 3$) compared with the control group (Control, $n = 3$). Bars represent SD. (E) Random blood glucose measurement showed decreased serum glucose in recipient mice (Transplant, $n = 3$) in comparison to control mice (Control, $n = 3$). Bars represent SD. (F) Similarly, serum IGF-I level was lower in recipient mice (Transplant, $n = 3$) compared with control mice (Control, $n = 3$). Bars represent SD. (G) Urine protein level was significantly decreased in recipient mice (Transplant, $n = 3$) compared with control mice (Control, $n = 3$). Bars represent SD. (H) Western blot analysis showed that expression of insulin receptor (IR) α , IR β , phosphatidylinositol 3-kinase (PI3-K) p85, and PI3-K p110 was down-regulated in kidney tissues of transplant recipient mice (Transplant, $n = 3$) compared with control mice (Control, $n = 3$). β -Actin was used as protein loading control.

(~ 2 -fold) as assessed by anti-proliferating cell nuclear antigen (PCNA) antibody staining (Figure S3D,E). In addition, PCNA-positive lymphoid cells were significantly increased (~ 2 -fold) in recipient mice compared with controls (Figure S3F).

Histologic studies of the spleen collected from 2 of 3 BMMSC-transplanted mice revealed a marked increase in B lymphocytes identified by B220 antibody immunostaining compared with the control mice (Figure S3G). Examination of the brain from these same transplanted mice showed a significantly decreased number of apoptotic cells in the hippocampus (Figure S4A) along with increased Purkinje cells (~ 2 -fold; Figure S4B) in the cerebellum and an increase (~ 3 -fold) in PCNA-positive ependymal cells of the choroid plexus (Figure S4C). In the liver, we observed a decreased number of degenerative hepatocytes and increased expression levels of ATPase (~ 1.5 -fold; Figure S4D,E). However, expression levels of mitochondria were found to be similar between BMMSC-transplanted and control mice (Figure S4F). Our data indicate that subcutaneous BMMSC transplantation offered a delay in aging-related degenerative changes in multiple organ systems of the recipients compared with their age-matched control mice.

Up-regulation of Klotho in BMMSC-transplanted mice

To determine the mechanism that may contribute to the life span extension by BMMSC transplantation, we examined expression level of Klotho, a circulating hormone capable of extending the life span of mice via regulation of IGF-I signaling pathway.¹⁸ In our study, we found that Klotho was significantly up-regulated (~ 2 -fold) in multiple organs of 3 BMMSC-transplanted mice, including epithelial cells lining the renal tubules (Figure 6A), kidney and brain tissues (Figure 6B,C), and peripheral blood (~ 1.5 -fold; Figure 6D). Systemically, 3 recipient mice that received BMMSC transplantation manifested significantly decreased serum glucose (~ 0.5 -fold) and IGF-I levels (~ 0.5 -fold) as well as a decreased urine protein level (~ 0.5 -fold) compared with control littermates (Figure 6E-G). Moreover, we found that several IGF-I signaling-associated molecules, including insulin receptors α and β and

phosphatidylinositol 3-kinase subunits p85 and p110, were down-regulated in kidney tissues of these recipient mice (Figure 6H). These results suggest that subcutaneous BMMSC transplantation is capable of up-regulating Klotho expression, which may contribute, at least in part, to the underlying altered antiaging physiology for the extended life span in the treated mice.

Discussion

Previous studies have identified that ectopically generated bone/marrow structures contain functional HSCs capable of rescuing impaired hematopoietic function in irradiated mice.⁴ Here, we demonstrate that subcutaneous transplantation of HA/TCP with human BMMSCs, not fibroblasts, can restore active hematopoiesis in immunocompromised mice. This evidence suggests that hematopoiesis, a fully active process that occurs in all marrow throughout the skeleton during early development, can be reinitiated at the ectopic site and presumably other bones, in this case the femurs and vertebrae, with increase in both myeloid and lymphoid components in adult immunocompromised mice. Although several growth factors, such as platelet-derived growth factor, vascular endothelial growth factor, and basic fibroblast growth factor, may contribute to BMMSC-associated ectopic bone marrow formation, the specific underlying mechanism remains unknown.⁴ We found that EPO-R, an early marker of BMMSCs and EPO-R/Stat5 pathway, is essential in the regulation of ectopic bone marrow formation in BMMSC transplants. Interestingly, very recent studies also suggested that EPO enhanced BMMSC-mediated cardiac tissue regeneration in a murine model of myocardial infarction.²⁹ A promising combined therapeutic modality using EPO and mesenchymal stem cells has been suggested in the neurogenesis of ischemic cerebral injury in rats.³⁰

In this study, we uncovered a potentially clinical impact in delaying the aging process using the innate physiologic process of bone marrow-mediated stem cell renewal and differentiation. Our

model of subcutaneous transplantation of BMMSC using a carrier provides a long-term engraftment of BMMSCs at the ectopic site at least 18 months, and these BMMSCs can be transferred to new hosts by secondary transplantation. The establishment of the functional ectopic hematopoietic organ unique to the subcutaneous transplantation, not standard BMMSC infusion approach, suggests a link between the presence of an organized BMMSC-hematopoietic organ, hematopoietic regeneration, and life span extension in mice. The low percentile of eGFP⁺ HSCs reflects stem cell homing to the primary BMMSC transplantations and subsequent engraftment in secondary transplants. The antiaging effect was probably attributed to the newly developed or reconstituted bone marrow organizing systems in recipients with capabilities to restore systemic immune functions, enhance tissue regeneration, and reverse aging-related degenerative changes at both cellular and organ levels.

The process of active generation of new hematopoietic marrow components, which mimics marrow-genesis observed in the early bone developmental stage, seen here at the ectopic subcutaneous hematopoietic organ in BMMSC/HA/TCP transplant mice, as well as other skeletal bones, appears to slow down as the animal ages and is an important aging-related degenerative phenotype with a broad systemic effect and therefore unsurprisingly affects the longevity of the transplant recipient. Although it has been suggested that regulating immune function is a potential approach in the manipulation of life span in lower organism model,³¹ up to date, there is no such study in the vertebrate species. Our established model of subcutaneous transplantation of BMMSC in immunocompromised mice will allow us to unfold the effect of BMMSC-mediated hematopoiesis restoration on life span enhancement and delayed degenerative changes in aging mice. We demonstrated that BMMSC transplantation resulted in elevated Klotho expression and suppression of IGF-I signaling in recipient mice. Because BMMSCs do not express Klotho in our system, we reasoned that BMMSC-mediated hematopoiesis may partly link to Klotho expression. Recently, the overexpression of Klotho, a circulating hormone that inhibits intracellular insulin and IGF-I signaling, has been implied in life span extension in mice.¹⁸ Although it is known that regulating immune function may manipulate life span,³¹ it is unknown how BMMSC transplantation resulted in elevated expression of Klotho. Until now, the identification of longevity-associated genes appears to involve the insulin receptor/IGF-I receptor pathway, by regulating cellular stress and caloric restriction in mice. In contrast, reduced IGF-I activity in humans is not associated with longevity. In humans, low IGF-I activity has been associated with an increased risk of developing cardiovascular disease and diabetes.³²⁻³⁵ In contrast, high IGF-I activity in humans is associated with an increased risk of developing cancer of the breast, prostate, lung, and colon.³⁶⁻³⁹ These findings suggest that multiple pathways contribute to the antiaging effects and the prolongation of life in complex organisms. Extending life span by BMMSC-organized hematopoietic marrow elements is physiologically complex and uniquely distinct from previously reported life

span alteration caused by a single gene or signaling pathway. Our approach, based on BMMSC-mediated reconstitution of the hematopoietic system resembling developmental marrow-genesis, allows further investigation in the broader systemic effects on multiple bone marrow-related cellular and organ systems without the need for genetic manipulation.

Previous attempts using allogenic BMMSCs to generate ectopic bone/marrow structure in regular mice were not successful because of the strong immune response in the subcutaneous area. Currently, isolation of autologous BMMSCs from mice remains a challenged task, partly because of lethality secondary to the small body size of the animal. Therefore, our study used beige Nude XidIII (*nu/nu*) mutant mice, the immunocompromised strain caused by a triple constitutive gene mutation (www.harlan.com/models/beigenude.asp), in which BMMSCs can be transplanted to generate ectopic bone and hematopoietic marrow. We recognize that our existing model has some limitation in the general antiaging effects in the normal aging rodent; however, up to date, this animal model still represents an advanced *in vivo* system than the most widely used *in vivo* models, such as *Caenorhabditis elegans*, and provides a testable paradigm for alleviating common age-related degenerations in several organ systems and enhancing survival in adult immunocompromised mice.

Acknowledgments

The authors thank Dr Marian Young and Ms Tina Kilts (National Institute of Dental and Craniofacial Research) for assistance with collection and maintenance of mice.

This work was supported by the National Institute of Dental and Craniofacial Research (grants R01DE017449 and R21 DE017632), National Institutes of Health, Department of Health and Human Services (S.S.), the California Institute for Regenerative Medicine (grant RN1-00572; S.S., A.L.), and in part by the Intramural Research Program of the National Institute of Dental and Craniofacial Research, National Institutes of Health.

Authorship

Contribution: T.Y., Y.M., and K.A. performed and designed the majority of the experiments and analyzed data; Y.B. and W.S. performed and analyzed the histologic and DEX data; S.G. and W.J.C. helped with experimental design and preparation of the manuscript; and A.L. and S.S. designed whole experiments and prepared the manuscript.

Conflict-of-interest disclosure: The authors declare no competing financial interests.

Correspondence: Songtao Shi, Center for Craniofacial Molecular Biology, University of Southern California, Health Sciences Campus, 2250 Alcazar Street, CSA103, Los Angeles, CA 90033; e-mail: songtaos@usc.edu.

References

- Friedenstein AJ, Chailakhyan RK, Latsinik NV, Panasyuk AF, Keiliss-Borok IV. Stromal cells responsible for transferring the microenvironment of the hemopoietic tissues: cloning *in vitro* and retransplantation *in vivo*. *Transplantation*. 1974; 17:331-340.
- Owen M, Friedenstein AJ. Stromal stem cells: marrow-derived osteogenic precursors. *Ciba Found Symp*. 1998;136:42-60.
- Prockop DJ. Marrow stromal cells as stem cells for nonhematopoietic tissues. *Science*. 1977;276: 71-74.
- Miura Y, Gao Z, Miura M, et al. Mesenchymal stem cell-organized bone marrow elements: an alternative hematopoietic progenitor resource. *Stem Cells*. 2006;24:2428-2436.
- Caplan AI. Adult mesenchymal stem cells for tissue engineering versus regenerative medicine. *J Cell Physiol*. 2007;213:341-247.
- Kuznetsov SA, Krebsbach PH, Satomura K, et al. Single-colony derived strains of human marrow stromal fibroblasts form bone after transplantation *in vivo*. *J Bone Miner Res*. 1997;12:1335-1347.
- Umezawa A, Maruyama T, Segawa K, Shadduck

- RK, Waheed A, Hata J. Multipotent marrow stromal cell line is able to induce hematopoiesis in vivo. *J Cell Physiol*. 1992;151:197-205.
8. Krebsbach PH, Kuznetsov SA, Satomura K, et al. Bone formation in vivo: comparison of osteogenesis by transplanted mouse and human marrow stromal fibroblasts. *Transplantation*. 1997;63:1059-1069.
 9. Batouli S, Miura M, Brahim J, et al. Comparison of stem-cell-mediated osteogenesis and dentinogenesis. *J Dent Res*. 2003;82:976-981.
 10. Quarto R, Mastrogiacomo M, Cancedda R, et al. Repair of large bone defects with the use of autologous bone marrow stromal cells. *N Engl J Med*. 2001;344:385-386.
 11. Fouillard L, Bensidhoum M, Bories D, et al. Engraftment of allogeneic mesenchymal stem cells in the bone marrow of a patient with severe idiopathic aplastic anemia improves stroma. *Leukemia*. 2003;17:474-476.
 12. Le Blanc K, Rasmuson I, Sundberg B, et al. Treatment of severe acute graft-versus-host disease with third party haploidentical mesenchymal stem cells. *Lancet*. 2004;363:1439-1441.
 13. Bartke A. Minireview: role of the growth hormone/insulin-like growth factor system in mammalian aging. *Endocrinology*. 2005;146:3718-3723.
 14. Geesaman BJ. Genetics of aging: implications for drug discovery and development. *Am J Clin Nutr*. 2006;83[suppl]:466S-469S.
 15. Bartke A, Brown-Borg H. Life extension in the dwarf mouse. *Curr Top Dev Biol*. 2004;63:189-225.
 16. Kenyon C. The plasticity of aging: insights from long-lived mutants. *Cell*. 2005;120:449-460.
 17. De Grey AD. Calorie restriction, post-reproductive life span, and programmed aging: a plea for rigor. *Ann N Y Acad Sci*. 2007;1119:296-305.
 18. Kurosu H, Yamamoto M, Clark JD, Pastor JV, et al. Suppression of aging in mice by the hormone Klotho. *Science*. 2005;309:1829-1833.
 19. Brown-Borg HM. Hormonal regulation of aging and life span. *Trends Endocrinol Metab*. 2003;14:151-153.
 20. Holzenberger M, Dupont J, Ducos B, et al. IGF-1 receptor regulates life span and resistance to oxidative stress in mice. *Nature*. 2003;421:182-187.
 21. Bartke A, Chandrashekar V, Dominici F, et al. Insulin-like growth factor 1 (IGF-1) and aging: controversies and new insights. *Biogerontology*. 2003;4:1-8.
 22. Barbieri M, Bonafè M, Franceschi C, Paolisso G. Insulin/IGF-I-signaling pathway: an evolutionarily conserved mechanism of longevity from yeast to humans. *Am J Physiol Endocrinol Metab*. 2003;285:E1064-E1071.
 23. Simmons PJ, Torok-Storb B. Identification of stromal cell precursors in human bone marrow by a novel monoclonal antibody, STRO-1. *Blood*. 1991;78:55-62.
 24. Shi S, Gronthos S. Perivascular niche of postnatal mesenchymal stem cells identified in human bone marrow and dental pulp. *J Bone Miner Res*. 2003;18:696-704.
 25. Miura Y, Miura M, Gronthos S, et al. Defective osteogenesis of the stromal stem cells predisposes CD18-null mice to osteoporosis. *Proc Natl Acad Sci U S A*. 2005;102:14022-14027.
 26. National Center for Biotechnology Information. GenBank. <http://www.ncbi.nlm.nih.gov/entrez/>. Accessed May 15, 2008.
 27. National Center for Biotechnology Information. GenBank. <http://www.ncbi.nlm.nih.gov/entrez/>. Accessed May 15, 2008.
 28. Arcasoy MO. The non-haematopoietic biologic effects of erythropoietin. *Br J Haematol*. 2008;141:14-31.
 29. Copland IB, Jolicœur EM, Gillis MA, et al. Coupling erythropoietin secretion to mesenchymal stromal cells enhances their regenerative properties. *Cardiovasc Res*. 2008;79:405-415.
 30. Esneault E, Pacary E, Eddi D, et al. Combined therapeutic strategy using erythropoietin and mesenchymal stem cells potentiates neurogenesis after transient focal cerebral ischemia in rats. *J Cereb Blood Flow Metab*. 2008;28:1552-1563.
 31. DeVeale B, Brummel T, Seroude L. Immunity and aging: the enemy within? *Aging Cell*. 2004;3:195-208.
 32. Juul A, Scheike T, Davidsen M, Gyllenberg J, Jørgensen T. Low serum insulin-like growth factor I is associated with increased risk of ischemic heart disease: a population-based case-control study. *Circulation*. 2002;106:939-944.
 33. Laughlin GA, Barrett-Connor E, Criqui MH, Kritzer Silverstein D. The prospective association of serum insulin-like growth factor I (IGF-I) and IGF-binding protein-1 levels with all cause and cardiovascular disease mortality in older adults: the Rancho Bernardo Study. *J Clin Endocrinol Metab*. 2004;89:114-120.
 34. Paolisso G, Tagliamonte MR, Rizzo MR, et al. Low plasma insulin-like growth factor-1 concentrations predict worsening of insulin-mediated glucose uptake in older people. *J Am Geriatr Soc*. 1999;47:1312-1318.
 35. Sandhu MS, Heald AH, Gibson JM, et al. Circulating concentrations of insulin-like growth factor-I and development of glucose intolerance: a prospective observational study. *Lancet*. 2002;359:1740-1745.
 36. Hankinson SE, Willett WC, Colditz GA, et al. Circulating concentrations of insulin-like growth factor-I and risk of breast cancer. *Lancet*. 1998;351:1393-1396.
 37. Chan JM, Stampfer MJ, Giovannucci E, et al. Plasma insulin-like growth factor-I and prostate cancer risk: a prospective study. *Science*. 1998;279:563-566.
 38. Lukanova A, Toniolo P, Akhmedkhanov A, et al. A prospective study of insulin-like growth factor-I, IGF-binding proteins-1, -2 and -3 and lung cancer risk in women. *Int J Cancer*. 2001;92:888-892.
 39. Giovannucci E, Pollak MN, Platz EA, et al. A prospective study of plasma insulin-like growth factor-1 and binding protein-3 and risk of colorectal neoplasia in women. *Cancer Epidemiol Biomarkers Prev*. 2000;9:345-349.